

This article was downloaded by:

On: 15 January 2011

Access details: *Access Details: Free Access*

Publisher *Taylor & Francis*

Informa Ltd Registered in England and Wales Registered Number: 1072954 Registered office: Mortimer House, 37-41 Mortimer Street, London W1T 3JH, UK



Journal of Experimental Nanoscience

Publication details, including instructions for authors and subscription information:

<http://www.informaworld.com/smpp/title~content=t716100757>

Synthesis and characterisation of $\text{In}(\text{OH})_3$ and In_2O_3 nanoparticles by sol-gel and solvothermal methods

Azadeh Askarnejad^a; Mina Iranpour^b; Nader Bahramifar^c; Ali Morsali^a

^a Department of Chemistry, Faculty of Sciences, Tarbiat Modares University, Tehran, Islamic Republic of Iran ^b Department of Chemistry, Payame Noor University, Abhar, Zanjan, Islamic Republic of Iran ^c Department of Chemistry, Payame Noor University, Sari, Islamic Republic of Iran

Online publication date: 07 July 2010

To cite this Article Askarnejad, Azadeh , Iranpour, Mina , Bahramifar, Nader and Morsali, Ali(2010) 'Synthesis and characterisation of $\text{In}(\text{OH})_3$ and In_2O_3 nanoparticles by sol-gel and solvothermal methods', *Journal of Experimental Nanoscience*, 5: 4, 294 – 301

To link to this Article: DOI: 10.1080/17458080903513292

URL: <http://dx.doi.org/10.1080/17458080903513292>

PLEASE SCROLL DOWN FOR ARTICLE

Full terms and conditions of use: <http://www.informaworld.com/terms-and-conditions-of-access.pdf>

This article may be used for research, teaching and private study purposes. Any substantial or systematic reproduction, re-distribution, re-selling, loan or sub-licensing, systematic supply or distribution in any form to anyone is expressly forbidden.

The publisher does not give any warranty express or implied or make any representation that the contents will be complete or accurate or up to date. The accuracy of any instructions, formulae and drug doses should be independently verified with primary sources. The publisher shall not be liable for any loss, actions, claims, proceedings, demand or costs or damages whatsoever or howsoever caused arising directly or indirectly in connection with or arising out of the use of this material.

Synthesis and characterisation of $\text{In}(\text{OH})_3$ and In_2O_3 nanoparticles by sol-gel and solvothermal methods

Azadeh Askarinejad^a, Mina Iranpour^b, Nader Bahramifar^c and Ali Morsali^{a*}

^aDepartment of Chemistry, Faculty of Sciences, Tarbiat Modares University, PO Box 14155-4838, Tehran, Islamic Republic of Iran; ^bDepartment of Chemistry, Payame Noor University, Abhar, Zanjan, Islamic Republic of Iran; ^cDepartment of Chemistry, Payame Noor University, Sari, Islamic Republic of Iran

(Received 12 June 2009; final version received 26 November 2009)

Indium hydroxide nanostructures were synthesised by sol-gel and hydrothermal processes from indium acetate and sodium hydroxide as precursors and polyvinyl alcohol, polyvinyl pyrrolidone or polydimethylsiloxane as stabilisers. Calcination of the $\text{In}(\text{OH})_3$ nanostructures at 500°C in air yielded In_2O_3 nanoparticles. The morphology, crystallinity and thermal behaviour of the obtained products of each method were investigated by X-ray diffraction, scanning electron microscopy and thermal gravimetry analysis and differential thermal analysis.

Keywords: indium hydroxide; nanostructure; sol-gel; hydrothermal

1. Introduction

Semiconductor nanostructures have been attracting increasing attention because of their exceptional properties, which differ from those of their bulk counterparts, and their potential applications in optoelectronic devices [1]. In_2O_3 is an important functional material. It has been widely used in photoelectronic thin films [2–4], gas sensors [5,6] and so on. Indium oxide is an important transparent conducting oxide (TCO) material that has applications in optoelectronics [7–9] and flat panel displays due to its high electrical conductivity and high optical transparency [10]. Since the first report of nanobelt structures of In_2O_3 in 2001 [11], there are some reports related to nanostructures of In_2O_3 [12–15]. Different methods have been used to produce different In_2O_3 nanostructures. Hydrothermal synthesis, as an important method of wet chemistry, has attracted lots of attention from materials scientists and chemists [16].

In this article, we present a facile method for preparation of In_2O_3 nanoparticles via a hydrothermal synthesis route and also a sol-gel technique. The products obtained under different conditions were characterised by X-ray powder diffraction (XRD), scanning electron microscopy (SEM) and thermal gravimetry analysis and differential thermal analysis (TG/DTA) methods and the results were compared with each other, and the effect

*Corresponding author. Email: morsali_a@modares.ac.ir

of different factors on size, morphology and crystallinity of the nanoparticles were investigated.

2. Experimental

In the sol-gel method, 0.58 g (2 mmol) indium acetate and 6 mmol NaOH or NH₃ were dissolved in 30 mL EtOH or H₂O as solvents. Then, 1 g PVA, PVP or PDMS were added to the solution. The solution was stirred and heated to become homogenous (sol) and then was converted to a viscose gel. The obtained gel was calcinated in a furnace by heating at 500°C and In₂O₃ nanoparticles resulted.

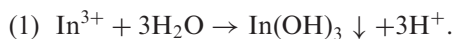
In the solvothermal procedure, 0.58 g (2mmol) indium acetate and 6 mmol (0.24 g) sodium hydroxide were dissolved in 15 mL EtOH, H₂O or a mixture of H₂O and EtOH. The solution was charged into a Teflon-lined stainless steel autoclave and heated at 150°C for 48 h or 24 h.

After the autoclave was cooled to room temperature, the product was filtered and dried and characterised as In(OH)₃. In(OH)₃ nanopowders were calcinated to 500°C to recrystallise to In₂O₃.

Table 1 shows the conditions of all reactions in detail. The products were analysed by XRD performed using a Philips diffractometer of X'pert company with monochromatised CuK_α radiation. The crystallite sizes of selected samples were estimated using the Scherrer method. TGA and DTA curves were recorded using a PL-STA 1500 device manufactured by Thermal Sciences. The samples were analysed with a SEM (LEO 1455 VP) with gold coating.

3. Results and discussion

In the hydrothermal process, In(OH)₃ nanopowders are prepared by the hydrolysis reaction of In³⁺ at 150°C, as described in reaction 1. The reaction mixture is heated above the boiling point of solvent in an autoclave and the sample is exposed to steam at high pressure. This procedure yields particles with nanometer scales. As-synthesised powders, depending on the synthesis technique used, they require subsequent heat treatment for dehydration, removal of organics and controlled crystallisation to form oxides with desirable structure and crystallite size. After calcination at 500°C nanoparticles of In₂O₃ are obtained by the reaction 2.



(2) $2\text{In}(\text{OH})_3 \xrightarrow{\text{calcination}} \text{In}_2\text{O}_3 + 3\text{H}_2\text{O}$. In the sol-gel process, hydrolysis and condensation of metal alkoxides occur. Metal alkoxides have the general formula M(OR)_x and an alkoxide ion is the conjugate base of an alcohol. The general synthesis of metal alkoxides involves the reaction of metal species with an alcohol. Metal alkoxides are good precursors because they readily undergo hydrolysis. The hydrolysis step replaces an alkoxide with a hydroxide group. In(OH)₃ is polymerised and forms In₂O(OH)₄ gelation, as described in reaction 3 and after calcination, surfactant decomposition and loss of solvent, nanoparticles of In₂O₃ are obtained (reaction 4).

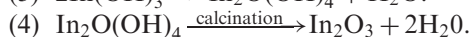
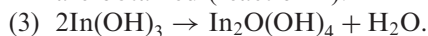


Table 1. Experimental conditions for the preparation of $\text{In}(\text{OH})_3$ and In_2O_3 nanostructures.

Reaction number	mmol of $\text{In}(\text{OAc})_2$	mmol of NaOH	Volume of solution	Solvent	Reaction time	Stabiliser	Product before calcination	Product after calcination	Method
1	2	6	15	H_2O	48 h		$\text{In}(\text{OH})_3$	In_2O_3	Hydrothermal
2	2	6	15	H_2O	24 h		$\text{In}(\text{OH})_3$	In_2O_3	Hydrothermal
3	2	6	15	EtOH	48 h		$\text{In}(\text{OH})_3$	In_2O_3	Solvothermal
4	2	6	15	EtOH	24 h		$\text{In}(\text{OH})_3$	In_2O_3	Solvothermal
5	2	6	15	$\text{H}_2\text{O} + \text{EtOH}$	48 h		$\text{In}(\text{OH})_3$	In_2O_3	Solvothermal
6	2	6	15	$\text{H}_2\text{O} + \text{EtOH}$	24 h		$\text{In}(\text{OH})_3$	In_2O_3	Solvothermal
7	2	6	30	EtOH		PVA	$\text{In}_2\text{O}(\text{OH})_4$	In_2O_3	Sol-gel
8	2	6	30	EtOH		PVP	$\text{In}_2\text{O}(\text{OH})_4$	In_2O_3	Sol-gel
9	2	6	30	H_2O		PVA	$\text{In}_2\text{O}(\text{OH})_4$	In_2O_3	Sol-gel
10	2	6	30	EtOH		PDMS	$\text{In}_2\text{O}(\text{OH})_4$	In_2O_3	Sol-gel

The XRD patterns of nanoparticles are shown in Figure 1. Figure 1(a) shows the XRD pattern of $\text{In}(\text{OH})_3$ synthesised by solvothermal method, reaction no. 4 (Table 1). These nanoparticles have shown good crystallinity because of the existence of sharp peaks in the XRD pattern. The phase purity of the as-prepared $\text{In}(\text{OH})_3$ nanoparticles is completely obvious and all diffraction peaks are perfectly indexed to cubic structure with lattice parameters of $a = 7.958 \text{ \AA}$ and $Z = 8$ and space group = $Pn3m$ which are in JCPDS card file no. 16-0161. No characteristic peaks of impurities are detected in the XRD pattern. The XRD patterns of all other products are the same as these patterns. The broadening of the peaks indicated that the particles were of nanometer scale. In a diffraction pattern, peak broadening is due to four factors: microstrains (deformations of the lattice), faulting (extended effects), crystalline domain size and domain size distribution. If we assume that analysed samples are free of strains and faulting, peak broadening is only due to crystalline domain size, D . D can then be calculated by the Scherrer formula [17], so it is always observed that the average size obtained by this formula is less than the one which is obtained from SEM and TEM images. Estimated from the Scherrer formula, $D = 0.891 \lambda / \beta \cos \theta$, where D is the average grain size, λ is the X-ray wavelength (0.15405 nm), θ and β are the diffraction angle and full-width at half maximum of an observed peak, respectively [1]; the average size of the particles of this sample was 58 nm, which is to some

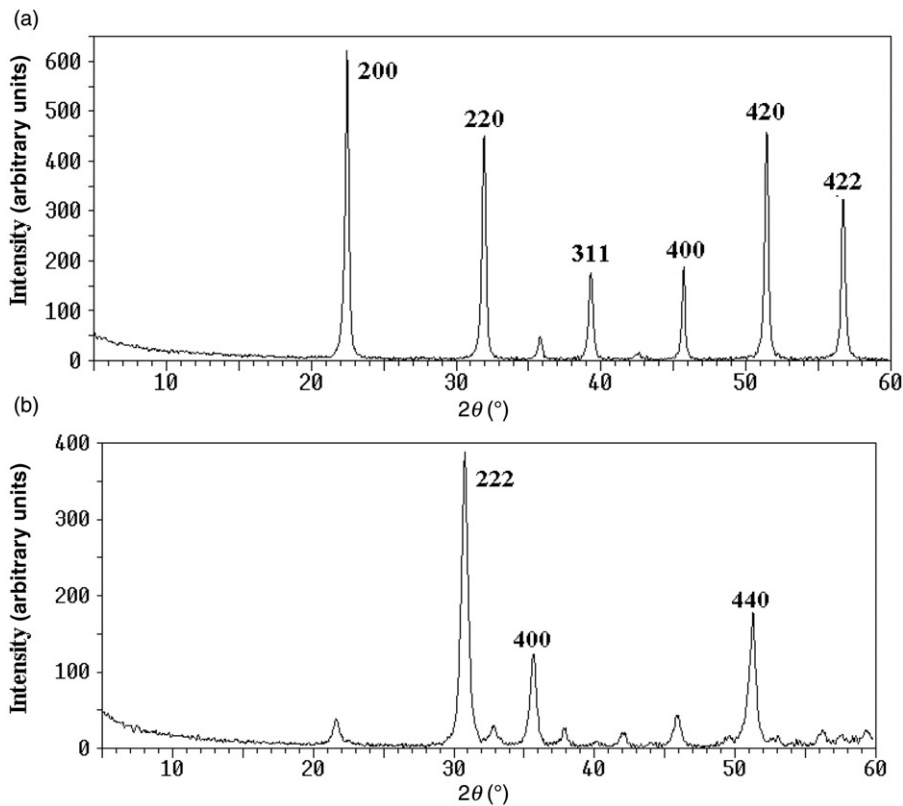


Figure 1. X-ray powder diffraction pattern of (a) $\text{In}(\text{OH})_3$ and (b) In_2O_3 .

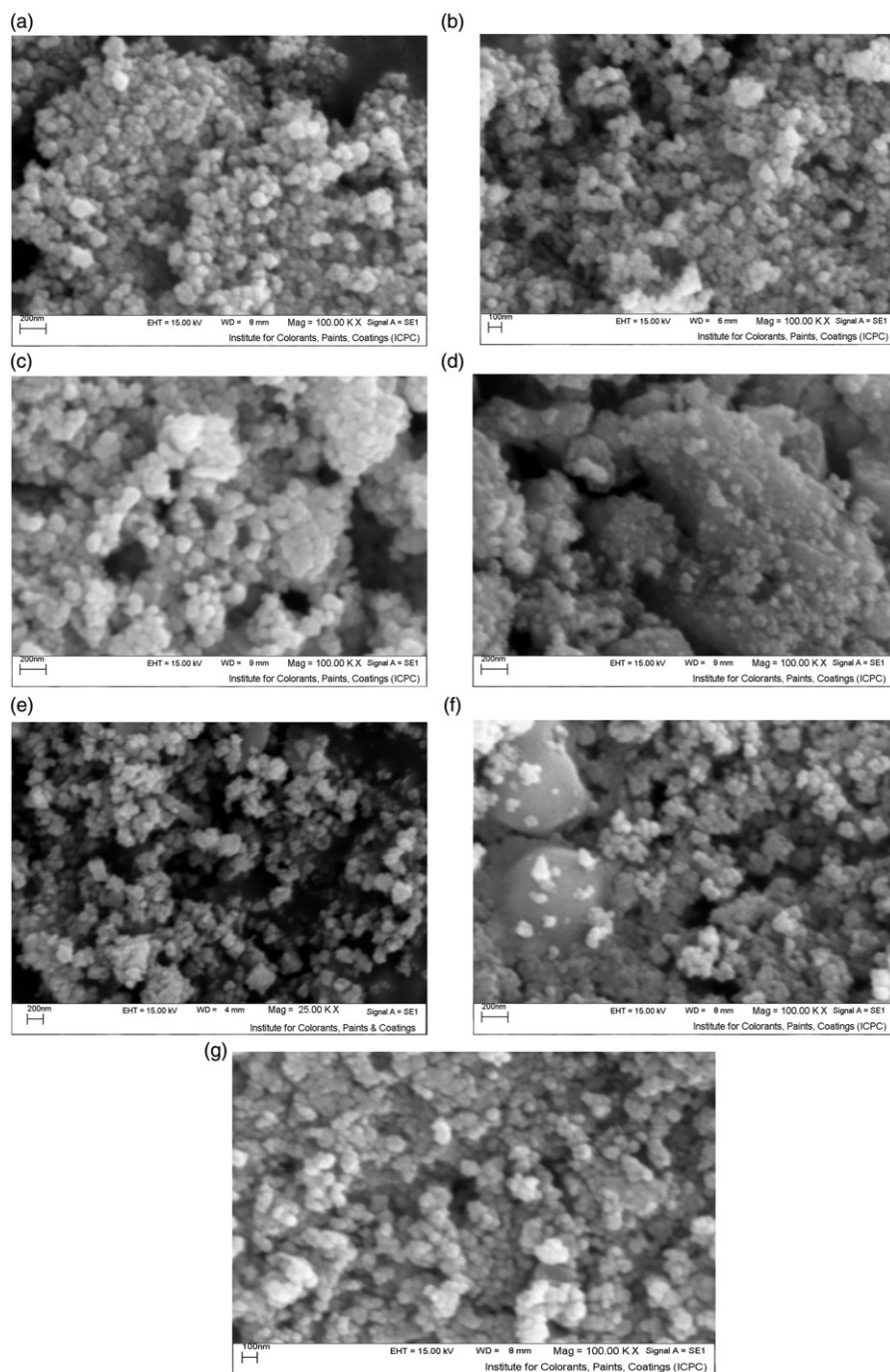


Figure 2. SEM images of (a) $\text{In}(\text{OH})_3$ (sample no. 4), (b) In_2O_3 (sample no. 4), (c) $\text{In}(\text{OH})_3$ (sample no. 2), (d) In_2O_3 (sample no. 2), (e) In_2O_3 (sample no. 7), (f) In_2O_3 (sample no. 8) and (g) In_2O_3 (sample no. 10).

extent in agreement with that observed from SEM images. Figure 1(b) shows the XRD pattern of In_2O_3 nanoparticles prepared by calcination of the $\text{In}(\text{OH})_3$ nanoparticles of reaction no. 4 (Table 1) and also In_2O_3 nanoparticles prepared via sol-gel route, reaction no. 10 (Table 1). All the peaks are corresponding to cubic structure with lattice constants $a = 10.118 \text{ \AA}$, $Z = 16$ and space group = 12_13 (JCPDS card file no. 44-1087). The average size of the nanoparticles of this sample, which is calculated from the Scherrer formula is 29.4 nm.

The SEM micrographs of the as-prepared $\text{In}(\text{OH})_3$ and In_2O_3 nanostructures are shown in Figure 2. Figure 2(a) shows the SEM image of $\text{In}(\text{OH})_3$ nanoparticles prepared by a solvothermal method using EtOH as solvent, and Figure 2(b) shows the In_2O_3 nanoparticles obtained by calcinating $\text{In}(\text{OH})_3$. Figure 2(c) and (d) show the SEM images of $\text{In}(\text{OH})_3$ and In_2O_3 nanoparticles prepared by a hydrothermal route. Figure 2(e), (f) and (g) show the SEM images of In_2O_3 nanoparticles prepared via sol-gel route by using PVA, PVP and PDMS as stabilisers, respectively. As it can be seen, there is no considerable difference in the morphology of the nanostructures obtained in different conditions. The In_2O_3 nanoparticles of sample no. 2 prepared by the hydrothermal process with the

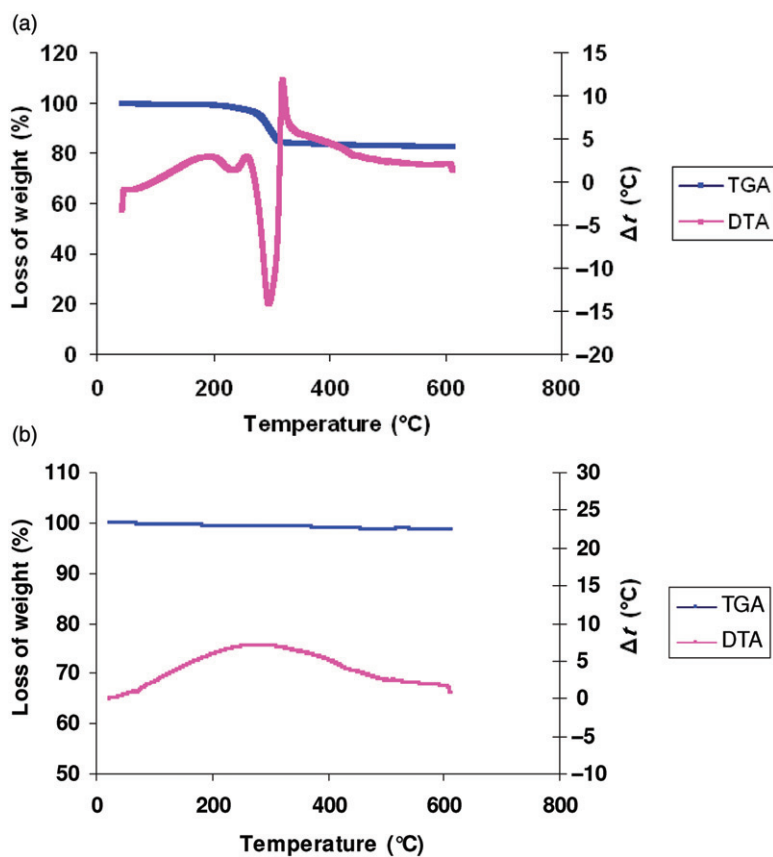


Figure 3. DTA and TGA diagrams of (a) $\text{In}(\text{OH})_3$ and (b) In_2O_3 nanoparticles.

details explained in Table 1, have smaller size than the other samples. The role of different polymers is not clear, but probably the best distribution of the particles is observed in sample no. 10, which is prepared by using PDMS. The average size of nanoparticles is about 50 nm.

Figure 3(a) shows the DTA and TGA curves of $\text{In}(\text{OH})_3$ recorded in static air atmosphere from ambient temperature to 700°C . A broad and strong endothermic peak was noticed at 240°C in the DTA curve, which can be assigned to decomposing of $\text{In}(\text{OH})_3$ and In_2O_3 crystallisation. In the TGA curve, a weight loss of 18% between 230 and 250°C which is assigned to decomposing of $\text{In}(\text{OH})_3$ to In_2O_3 , was noticed. Figure 3(b) shows the DTA and TGA curves of In_2O_3 nanoparticles obtained by calcinations. As it can be seen, there is not any noticeable loss of weight.

In recent years, many methods such as co-precipitation method and thermal evaporation method [12], non-aqueous sol-gel method [13], CVD route [14], glass crystallisation [15] and microemulsion-mediated hydrothermal synthesis [1] have been used for preparing different shapes of In_2O_3 nanostructures. The methods reported in this article are very simple and rapid and yield uniform nanoparticles of In_2O_3 and $\text{In}(\text{OH})_3$ with good size distribution.

4. Conclusion

In summary, a simple solvothermal and sol-gel route by modifying the different parameters have been used to successfully synthesise the nanoparticles of In_2O_3 and $\text{In}(\text{OH})_3$. These methods have been used to synthesise other oxide nanoparticles so far [18–20]. All the results obtained by SEM images and XRD, TG/DTA analyses confirm the production of uniform, sphere-like nanostructures of these compounds. To our knowledge, these methods with the present conditions have not been used for preparing these nanostructures so far. The investigated factors did not have special effects on morphology, size and crystallinity of the nanostructures.

Acknowledgements

This work was supported by the Tarbiat Modares and Payame Noor Universities.

References

- [1] J. Yang, C. Lin, Z. Wang, and J. Lin, *In(OH)₃ and In₂O₃ nanorod bundles and spheres: Microemulsion-mediated hydrothermal synthesis and luminescence properties*, *Inorg. Chem.* 45 (2006), pp. 8973–8979.
- [2] M. Kamei and Y. Shigesato, *Origin of characteristic grain-subgrain structure of tin-doped indium oxide films*, *Thin Solid Films* 295 (1995), pp. 38–45.
- [3] N.R. Armstrong, C. Carter, C. Donley, A. Simmonds, P. Lee, M. Brumbach, B. Kippelen, B. Domercq, and S. Yoo, *Interface modification of ITO thin films: Organic photovoltaic cells*, *Thin Solid Films* 445(2) (2003), pp. 342–352.
- [4] R. Schiller, G. Battistig, and J. Rabani, *Reversible electrochemical coloration of indium tin oxide (ITO) in aqueous solutions*, *Radiat. Phys. Chem.* 72(2–3) (2005), pp. 217–223.

- [5] J. Zhang, J. Hu, Z.Q. Zhu, H. Gong, and S.J. O'Shea, *Quartz crystal microbalance coated with sol-gel-derived indium-tin oxide thin films as gas sensor for NO detection*, *Colloids Surf., A* 236(1–3) (2004), pp. 23–30.
- [6] N.G. Patel, K.K. Makhija, and C.J. Panchal, *Fabrication of carbon tetrachloride gas sensors using indium tin oxide thin films*, *Sens. Actuator, B* 23(1) (1995), pp. 49–53.
- [7] B.Y. Pines, *J. Tech. Phys. (USSR)* 26 (1956), p. 2086.
- [8] Y.E. Geguzin, *Surface diffraction and spreading*, Nauka, Moscow, 1969, p. 11.
- [9] Ya. E. Geguzin, *Physics of Sintering*, Nauka, Moscow, 1984.
- [10] E. Saiz, A.P. Tomsia, and K. Suganuma, *Wetting and strength issues at Al/ α -alumina interfaces*, *J. Eur. Ceram. Soc.* 23 (2003), pp. 2787–2796.
- [11] Z.W. Pan, Z.R. Dai, and Z.L. Wang, *Nanobelts of semiconducting oxides*, *Science* 291 (2001), pp. 1947–1949.
- [12] J.M. Kim, J.K. Park, K.N. Kim, C.H. Kim, and H.G. Jang, *Synthesis of In_2O_3 nano-materials with various shapes*, *Curr. Appl. Phys.* 6S1 (2006), pp. e198–e201.
- [13] G. Neri, A. Bonavita, G. Micali, G. Rizzo, N. Pinna, and M. Niederberger, *In_2O_3 and Pt- In_2O_3 nanopowders for low temperature oxygen sensors*, *Sens. Actuator B* 127 (2007), pp. 455–462.
- [14] Y. Zhanga, H. Agoa, J. Liub, M. Yumuraa, K. Uchidaa, S. Ohshimaa, S. Iijimaa, J. Zhub, and X. Zhang, *The synthesis of In, In_2O_3 nanowires and In_2O_3 nanoparticles with shape-controlled*, *J. Cryst. Growth* 264 (2004), pp. 363–368.
- [15] R. Garkova, G. Völksch, and C. Rüssel, *In_2O_3 and tin-doped In_2O_3 nanocrystals prepared by glass crystallization*, *J. Non-Cryst. Solids* 352 (2006), pp. 5265–5270.
- [16] Y. Chen, R. Yu, Q. Shi, J. Qin, and F. Zheng, *Hydrothermal synthesis of hexagonal ZnO clusters*, *Mater. Lett.* 61 (2007), pp. 4438–4441.
- [17] A. Weibel, R. Bouchet, F. Boule'h, and P. Knauth, *The big problem of small particles: A comparison of methods for determination of particle size in nanocrystalline anatase powders*, *Chem. Mater.* 17 (2005), pp. 2378–2385.
- [18] N. Soltanzadeh and A. Morsali, *Synthesis and characterization nano-structured bismuth(III) oxide from a new nano-sized bismuth(III) supramolecular compound*, *Polyhedron* 28 (2009), pp. 1343–1347.
- [19] A. Aslani and A. Morsali, *Sonochemical synthesis of nano-sized metal-organic lead(II) polymer: A precursor for the preparation of nano-structured lead(II) iodide and lead(II) oxide*, *Inorgan. Chim. Acta* 362 (2009), pp. 5012–5016.
- [20] A. Askarnejad and A. Morsali, *Synthesis and characterization of $CdCO_3$ and CdO nanoparticles by using a sonochemical method*, *Mater Lett.* 62 (2008), pp. 478–482.